NEURAL REGENERATION RESEARCH
Volume 8, Issue 21, July 2013

www.nrronline.org

doi:10.3969/j.issn.1673-5374.2013.21.002 [http://www.nrronline.org; http://www.sjzsyj.org]
Zhang L, Yang J, Cao YP. What is the new target inhibiting the progression of Alzheimer's disease? Neural Regen Res. 2013;8(21):1938-1947.

What is the new target inhibiting the progression of Alzheimer's disease?

Lin Zhang[1], Jing Yang[2], Yunpeng Cao[1]

1 *Department of Neurology, First Affiliated Hospital of China Medical University, Shenyang 110001, Liaoning Province, China*
2 *Provincial Key Laboratory of Cardiovascular and Cerebrovascular Drug Basic Research, Liaoning Medical University, Jinzhou 121001, Liaoning Province, China*

Research Highlights

(1) We investigated the mechanism of action of striatal-enriched phosphatase 61 at the behavioral and signaling molecule levels, using *in vivo* and *in vitro* models. We discussed the relationship of striatal-enriched phosphatase 61 with transgene and N-methyl-D-aspartate receptor 2B, and lyzed the molecular mechanism by which striatal-enriched phosphatase 61 regulates N-methyl-D-aspartate receptor 2B transport.
(2) Spatial learning and memory deficits in Alzheimer's disease may be associated with disturbed N-methyl-D-aspartate receptor 2B transport caused by striatal-enriched phosphatase 61.
RNA silencing can effectively inhibit striatal-enriched phosphatase 61 target gene expression and can be used to investigate the function and involvement of striatal-enriched phosphatase 61 in the pathogenesis of Alzheimer's disease.
(3) This study provides a basic reference for gene therapy for Alzheimer's disease using striatal-enriched phosphatase 61.

Abstract

To stop the progression of Alzheimer's disease in the early stage, it is necessary to identify new therapeutic targets. We examined striatal-enriched phosphatase 61 expression in the brain tissues of 12-month-old APPswe/PSEN1dE9 transgenic mice. Immunohistochemistry showed that al-enriched phosphatase 61 protein expression was significantly increased but phosphorylated N-methyl-D-aspartate receptor 2B levels were significantly decreased in the cortex and hippocampus of APPswe/PSEN1dE9 transgenic mice. Western blotting of a cell model of Alzheimer's disease consisting of amyloid-beta peptide (1–42)-treated C57BL/6 mouse cortical neurons *in vitro* showed that valeric acid (AP5), an N-methyl-D-aspartate receptor antagonist, significantly inhibited amyloid-beta 1–42-induced increased activity of striatal-enriched phosphatase 61. In addition, the phosphorylation of N-methyl-D-aspartate receptor 2B at Tyr1472 was impaired in amyloid-beta 1–42-treated cortical neurons, but knockdown of striatal-enriched phosphatase 61 enhanced the phosphorylation of N-methyl-D-aspartate receptor 2B. Collectively, these findings indicate that striatal-enriched phosphatase 61 can disturb N-methyl-D-aspartate receptor transport and inhibit the progression of learning and study disturbances induced by Alzheimer's disease. Thus, al-enriched phosphatase 61 may represent a new target for inhibiting the progression of Alzheimer's disease.

Key Words

neural regeneration; brain injury; neurodegeneration; Alzheimer's disease; striatal-enriched phosphatase 61; amyloid-beta peptide; N-methyl-D-aspartate receptor; GluN2B; RNA interference; immunohistochemistry; western blot; neuroregeneration

Lin Zhang, Studying for doctorate, Associate chief physician.

Corresponding author: Yunpeng Cao, Professor, Doctoral supervisor, Department of Neurology, First Affiliated Hospital of China Medical University, Shenyang 110001, Liaoning Province, China, ypengcao@yahoo.com.

Received: 2013-04-06
Accepted: 2013-06-18
(N201302034)

Acknowledgments: We thank Shao YG, Department of Cell Biology, Key Laboratory of Cell Biology, Ministry of Public Health, Key Laboratory of Medical Cell Biology, Ministry of Education, China Medical University, for help with manuscript preparation.

Author contributions: Zhang L designed the study, performed experiments and wrote the manuscript. Yang J assisted in directing the experiments. Cao YP directed the research and supervised the manuscript writing. All authors read and approved the final manuscript.

Conflicts of interest: None declared.

Ethical approval: All experiments were conducted in accordance with the Jeju National University Guide for the Care and Use of Laboratory Animals (JNU-ACUCC No. 2010025).

Author statements: The manuscript is original, has not been submitted to or is not under consideration by another publication, has not been previously published in any language or any form, including electronic, and contains no disclosure of confidential information or authorship/patent application disputations.

INTRODUCTION

Alzheimer's disease is characterized by the accumulation of amyloid-beta (Aβ) peptide in brains, a process that has been implicated in the progression of the disease[1]. One hypothesis for the pathophysiology of Alzheimer's disease is that soluble forms of Aβ disrupt synaptic function[2-3]. Amyloid plaque formation occurs subsequent to the loss of synaptic function[4], suggesting that synaptic perturbations are an earlier target of Aβ. The mechanisms underlying Aβ-induced reductions in synaptic function remain a focus of intense research.

Striatal-enriched phosphatase 61 ($STEP_{61}$; also known as protein tyrosine phosphatase non-receptor 5 (PTPN5)) is a brain-specific tyrosine phosphatase targeted to synaptic compartments in the striatum, hippocampus, cortex, and related brain regions[5]. Alternative splicing produces various STEP family members, and both cytosolic ($STEP_{46}$) and membrane-associated ($STEP_{61}$) variants exist[6-7]. STEP opposes the development of synaptic strengthening by dephosphorylating and inactivating key signaling proteins including the mitogen-activated protein kinases extracellular-regulated kinase 1/2 and p38[8], and the tyrosine kinase Fyn. STEP also dephosphorylates the GluR2 subunit of the α-amino-3-hydroxy-5-methyl-4-isoxazolepropionic acid receptor and the GluN2B subunit of the N-methyl-D-aspartate (NMDA) receptor, leading to internalization of the GluN1/GluN2B and GluR1/GluR2 receptors. STEP levels and activity are regulated by phosphorylation, local translation, ubiquitination, degradation and proteolytic cleavage[9-10].

Glutamatergic signaling through NMDA receptors is required for synaptic plasticity. Disruptions in glutamatergic signaling are proposed to contribute to behavioral and cognitive deficits[11]. Recent evidence suggests that glutamate receptors are dysregulated by Aβ oligomers, resulting in disruption of glutamatergic synaptic transmission, which parallels early cognitive deficits[12]. NMDA receptors are heteromultimeric complexes comprised of at least two types of subunits, the principal subunit GluN1 and the modulatory subunit GluN2A-D[13]. The GluN2B receptor has been identified as a major tyrosine phosphorylated protein in the postsynaptic density and plays a key role in the signal transduction pathways for NMDA receptor activation[14]. Some studies have suggested a role for tyrosine phosphorylation of GluN2B in the enhancement of synaptic efficacy, and thus, in the development of central sensitization[15], an important synaptic process in Alzheimer's disease research.

Furthermore, NMDA-receptor-mediated glutamate excitotoxicity plays a major role in Aβ-induced neuronal death. It is thought that NMDA receptors represent a promising target for preventing the progression of Alzheimer's disease[16]. Excitotoxic neuronal cell death is mediated in part by overactivation of NMDA-type glutamate receptors, which results in excessive Ca^{2+} influx through the receptor's associated ion channel. However, whether $STEP_{61}$ affects phosphorylation of GluN2B *via* NMDA receptor has not been examined.

In the present study, we characterized the cognitive deficits and the detailed $STEP_{61}$-related pathologies in the cerebral cortex and hippocampus in 12-month-old APPswe/PSEN1dE9 transgenic (APP/PS1) mice, a well-established transgenic mouse model of Alzheimer's disease. We further investigated the mechanisms by which $STEP_{61}$ regulates Aβ-mediated phosphorylation of GluN2B *via* NMDA receptors in an Alzheimer's disease cell model.

RESULTS

Quantitative analysis of experimental animals

Eight 12-month-old male APP/PS1 mice were selected, and another eight 12-month-old male wild-type mice (C57BL/6) were used as controls. Sixteen mice were involved in the final analysis.

Spatial learning and memory deficits in APP/PS1 transgenic mice

All APP/PS1 mice used in our study were genotyped using a standardized PCR assay on tail DNA, which confirmed that the mice were APP/PS1 mice (Figure 1). The spatial learning and memory functions of all mice were assessed by Morris water maze. During the training acquisition phase, as shown in Figure 2C, both APP/PS1 transgenic mice and wild-type mice readily learned the location of the hidden platform, as shown by a decrease in the escape latency over training days. One-way analysis of variance results revealed a significant main effect of genotype on the escape latency measured over all days ($P < 0.001$), suggesting that APP/PS1 mice required a significantly longer time to locate the hidden platform relative to wild-type mice, and that spatial learning was impaired in these transgenic mice. Moreover, there was no significant effect of genotype on swimming speed measured over all training days ($P > 0.05$; Figure 2D), suggesting that mean swimming speed did not differ between transgenic and control mice during the spatial learning training phase in the water maze. This indicates that the spatial learning deficits in transgenic mice did not result from their motor deficits.

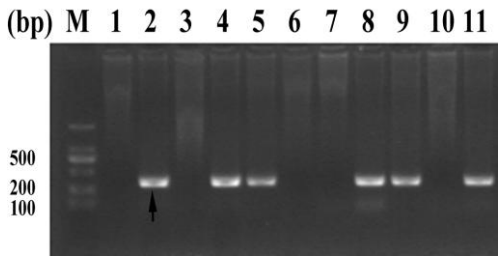

Figure 1 Amplification products of the APP gene from tail DNA.

The arrow indicates the location of the corresponding PCR-signal (270 bp). M: Marker of fragment lengths; lanes 1, 3, 6, 7, 10 represent wild-type mice; lanes 2, 4, 5, 8, 9, 11 represent APP/PS1 mice. Lanes 2, 4, 5, 8, 9, 11 show that the PCR results were as expected. Negative controls were PCRs using DNA from wild-type mice (lanes 1, 3, 6, 7, 10)

Spatial memory was evaluated in all mice by probe trial performed 24 hours after the last training session. APP/PS1 mice spent less time in the target quadrant than wild-type mice ($P < 0.001$), indicating impaired spatial memory retention in these transgenic mice (Figure 2A, B, and E). Moreover, the visible platform trails in the water maze revealed no significant differences in escape latency between APP/PS1 mice and wild-type mice ($P > 0.05$; Figure 2F). This implies that the learning and memory impairments of APP/PS1 mice were not caused by vision and motor dysfunctions or a lack of motivation. In summary, 12-month-old APP/PS1 mice showed evident hippocampus-dependent spatial learning and memory deficits in the water-maze.

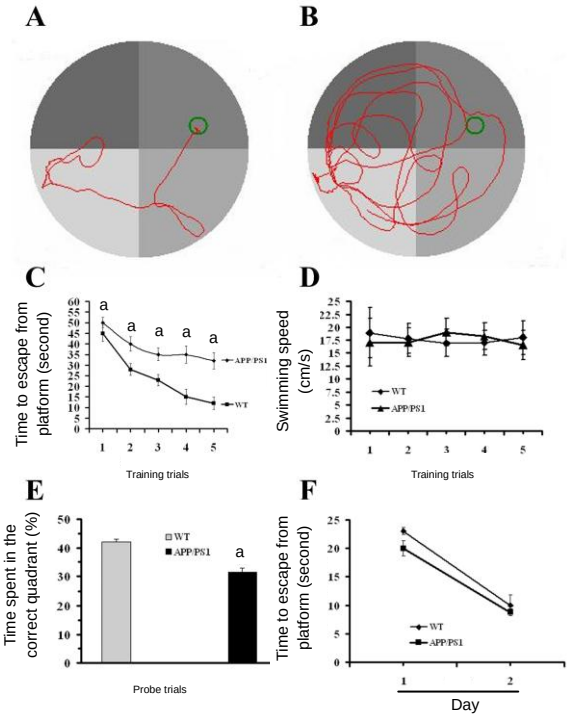

Figure 2 Spatial learning and memory deficits in APPswe/PSEN1dE9 (APP/PS1) transgenic mice.

Representative swim traces for each group in probe trials: (A) Wild-type (WT) mice. (B) APP/PS1 mice.

(C) In the hidden platform trials in the Morris water maze, APP/PS1 transgenic mice had significantly longer escape latencies than wild-type mice, as demonstrated by a significant effect of genotype. All results are expressed as the mean for each group (six mice for each group). The difference between groups was analyzed using one-way analysis of variance and Student-Newman-Keuls *post hoc* tests. $^{a}P < 0.001$, *vs*. wild-type group.

(D) Swimming speed in training trials showed no difference in motor function in each group ($P > 0.05$).

(E) Percent goal quadrant dwell time in the probe trials. In the probe trial, 24 hours after the last training session, the transgenic mice spent less time in the target quadrant compared with wild-type mice. All results are expressed as the mean for each group (six mice for each group). The difference between groups was analyzed using one-way analysis of variance and Student-Newman-Keuls *post hoc* tests. $^{a}P < 0.001$, *vs*. wild-type mice.

(F) No significant differences were detected between APP/PS1 and wild-type mice in the visible platform trials ($P > 0.05$). All tests were performed at least three times to ensure reproducibility.

Expression of $STEP_{61}$ in the cortex and hippocampus of APP/PS1 transgenic mice

To assess the distribution of $STEP_{61}$ in the cortex and

hippocampus, we performed immunohistochemistry analyses. Dense staining for $STEP_{61}$ was observed in the cortex and hippocampal CA1 region of APP/PS1 transgenic mice (Figure 3A). The $STEP_{61}$ HSCOREs in the cortex and hippocampal CA1 region from APP/PS1 mice were significantly higher than those in the same region from wild-type controls (APP/PS1: cortex = 1.64 ± 0.76, hippocampus = 1.83 ± 0.61; wild-type: cortex = 0.89 ± 0.44, hippocampus = 0.94 ± 0.35; $P = 0.003$ and $P = 0.000$, respectively; Figure 3B).

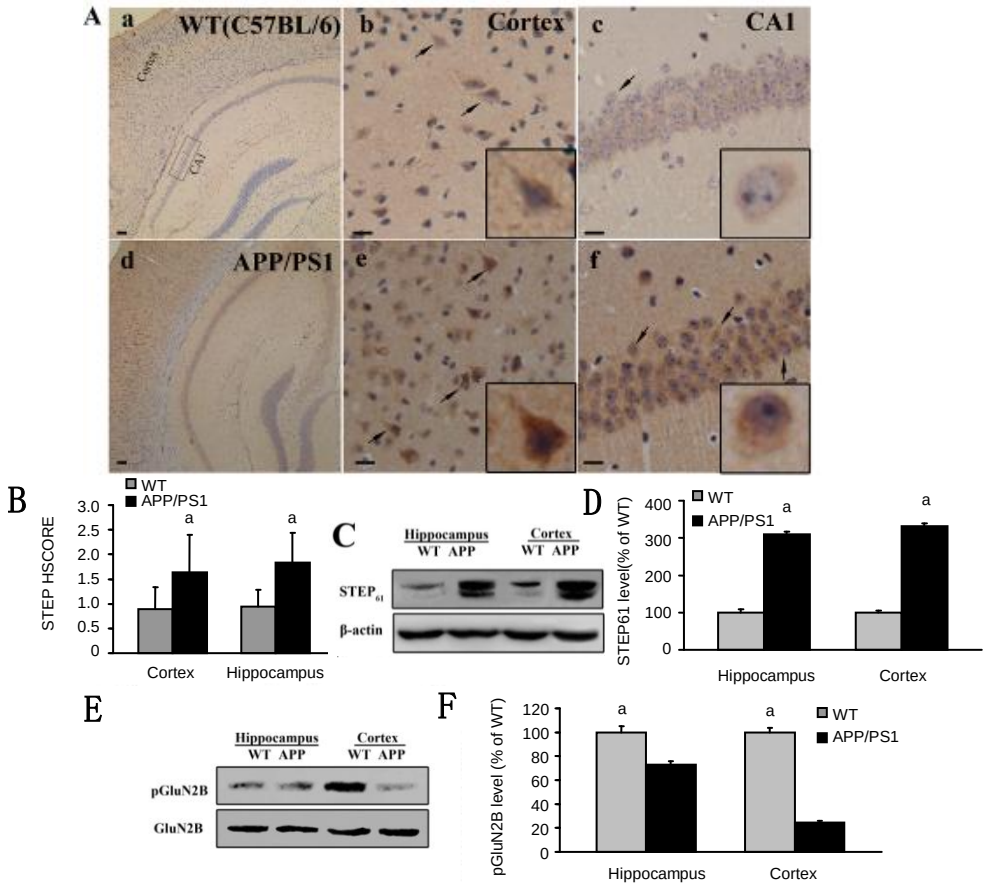

Figure 3 Expression of STEP61 in the cortex and hippocampus from APP/PS1 transgenic mouse brains.

(A) $STEP_{61}$ expression in the cortex and hippocampal CA1 region (immunohistochemistry). In contrast to less immunoreactivity in the wild-type (C57BL/6) mouse brain (a, b, c), more neurons were strongly stained in the APP/PS1 transgenic mouse brain (d, e, f). a, d: ×100, scale bars = 50 μm; b, c, e, f: × 200, scale bars = 25 μm. Arrows indicate STEP61-positive cells. Insets: high magnification (×400) of $STEP_{61}$-positive cells.

(B) $STEP_{61}$ HSCOREs in the cortex and hippocampal CA1 region. The $STEP_{61}$ HSCOREs in the cortex and hippocampal CA1 region from APP/PS1 mice were significantly higher than those in the same region from wild-type controls ($^aP < 0.01$, *vs.* wild-type mice, one-way analysis of variance and Student-Newman-Keuls *post hoc* tests; $STEP_{61}$ HSCOREs from five randomly selected sections). The HSCORE was calculated using two indices, proportion (Pí) and intensity (í). Pí was estimated after taking into account the percentage of positive cells. í was judged as 0 (no staining), or 1^+ (light brown staining), or 2^+ (brown staining), or 3^+ (heavy brown staining). The $STEP_{61}$ HSCORE was derived by summing the proportion of cells stained at each intensity, multiplied by the intensity of staining. HSCORE = $\sum$Pí × í.

(C) Immunoblotting and quantitation of $STEP_{61}$ levels (61 kDa) normalized to β-actin levels (42 kDa).

(D) $STEP_{61}$ levels were significantly increased in APP/PS1 mice brains compared with wild-type controls. Results are presented as percentages of the absorbance for wild-type controls. ($^aP < 0.001$, *vs*. wild-type mice; mean ± SD of eight mice for each group; one-way analysis of variance and Student-Newman-Keuls *post hoc* tests).

(E) pGluN2B levels (190 kDa) were analyzed in APP/PS1 transgenic mice. Equal amounts of protein from each sample were processed for immunoblot analysis using anti-pGluN2B, GluN2B antibodies.

(F) Quantitative analysis results for levels of pGluN2B. Results are presented as percentages of the absorbance for wild-type controls ($^aP < 0.001$, *vs*. wild-type mice. mean ± SD of eight mice for each group; one-way analysis of variance and Student-Newman-Keuls *post hoc* tests). All tests were performed at least three times to ensure reproducibility.

APP/PS1: APPswe/PSEN1dE9e; HSCORE: histological score.

We also performed western blot analyses to examine $STEP_{61}$ protein levels in synaptosomes in the hippocampus and cortex from APP/PS1 transgenic mice. The results showed that $STEP_{61}$ levels were significantly elevated in the hippocampus and cortex of APP/PS1 mice compared with the same brain regions in wild-type mice (Figure 3C). Quantitative analysis revealed that the $STEP_{61}$ level was significantly increased in the hippocampus of APP/PS1 mice compared with wild-type controls ($P < 0.001$; Figure 3C). $STEP_{61}$ levels were markedly increased in the cortex of APP/PS1 mice compared with wild-type control mice ($P < 0.001$; Figure 3C). We next examined the level of pGluN2B in the hippocampus and cortex in APP/PS1 mice compared with wild-type mice (Figure 3D). Notably, as in other Alzheimer's disease mouse models, the genotype significantly affected the level of pGluN2B. Student-Newman-Keuls *post hoc* tests revealed that basal expression of pGluN2B was reduced in APP/PS1 mice relative to wild-type mice ($P < 0.001$). These results reveal increased $STEP_{61}$ levels and decreased pGluN2B levels in the middle-aged APP/PS1 mouse brain.

RNAi silencing of $STEP_{61}$ decreases $STEP_{61}$ mRNA levels in cortical neurons

Cells were harvested 48 hours after transfection with $STEP_{61}$ siRNA and non-silencing siRNA, and were subjected to real-time reverse transcription-PCR analysis. The level of mRNA for $STEP_{61}$ was decreased by 83% in cells transfected with $STEP_{61}$ siRNA compared with the level in cells transfected with the non-silencing control siRNA (Figure 4A). We then examined whether RNAi silencing of $STEP_{61}$ could affect the viability of cortical neurons incubated with $A\beta_{1–42}$ 1 μmol/L for 1 hour. Cells were treated with $A\beta_{1–42}$ before transfection with $STEP_{61}$ RNAi for 48 hours. MTT analysis revealed that the cell viabilities were all dramatically increased in cortical neurons treated with $STEP_{61}$ siRNA as compared with controls (Figure 4B).

$STEP_{61}$ protein levels in $A\beta_{1–42}$-induced cortical neurons

The Aβ-induced increase in $STEP_{61}$ levels and the amount of dephosphorylated $STEP_{61}$ in cortical neurons was mediated by the NMDA receptor; RNAi silencing of $STEP_{61}$ increased pGluN2B levels in Aβ-treated cortical neurons.

We then investigated the effects of $A\beta_{1–42}$ on $STEP_{61}$ levels. Previous studies have shown that $STEP_{61}$ is present as a doublet and that the upper band (phosphorylated form) constitutes the principal component of the doublet under basal conditions[7]. Immunoblotting revealed a marked increase in $STEP_{61}$ levels by 225 ± 8.9% following $A\beta_{1–42}$ treatment ($P < 0.001$; Figure 5B). $A\beta_{1–42}$ treatment reduced the proportion of phosphorylated $STEP_{61}$ (phosphorylated/total $STEP_{61}$) to 72% of the control level ($P < 0.001$; Figure 5C; the proportion of dephosphorylated $STEP_{61}$ was significantly increased). Pretreatment with the NMDA receptor antagonist valeric acid (AP5) before treatment with $A\beta_{1–42}$ inhibited the increase in STEP levels and reduced proportion of dephosphorylated $STEP_{61}$ ($P < 0.001$; Figure 5C). In contrast, pretreatment with the non-NMDA receptor antagonist CNQX failed to inhibit the increase in STEP levels and activation. Next, western blot analysis demonstrated a significant reduction in pGluN2B levels after $A\beta_{1–42}$ treatment compared with controls ($P < 0.001$). However, the decreased GluN2B phosphorylation was significantly restored after treatment of cells with $STEP_{61}$ siRNA ($P < 0.001$; Figure 5D, E). These results suggest that NMDA receptor activity is necessary for the Aβ-induced increase in $STEP_{61}$ expression and activation, that $STEP_{61}$ negatively regulates Aβ-mediated phosphorylation, and that it possibly also regulates the activity of GluN2B.

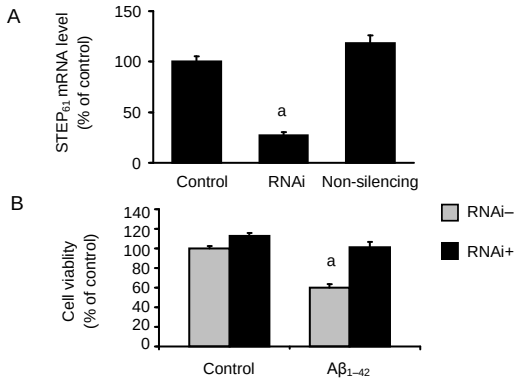

Figure 4 RNAi silencing of Striatal-enriched phosphatase 61 ($STEP_{61}$) decreased mRNA levels of $STEP_{61}$ and increased cell viability in cortical neurons.

(A) Cortical neurons were transfected with $STEP_{61}$ siRNA or with non-silencing siRNA, and harvested at 48 hours. Real-time reverse transcription-PCR results showed that mRNA absorbance of $STEP_{61}$ was significantly decreased in $STEP_{61}$ siRNA-treated cells compared with non-silencing controls ($^aP < 0.001$, *vs*. non-silencing controls; mean ± SD, $n = 5$ wells for each group; one-way analysis of variance and Student-Newman-Keuls *post hoc* tests).

(B) MTT analyses detected the effects of $STEP_{61}$ RNAi silencing on the viability of cortical neurons treated with amyloid-beta ($A\beta_{1–42}$) 1 μmol/L for 1 hour. $STEP_{61}$ siRNA treatments increased cell viability *vs*. controls ($^aP < 0.001$, *vs*. controls, mean ± SD, $n = 8$; one-way analysis of variance and Student-Newman-Keuls *post hoc* tests).

All tests were performed at least three times to ensure reproducibility.

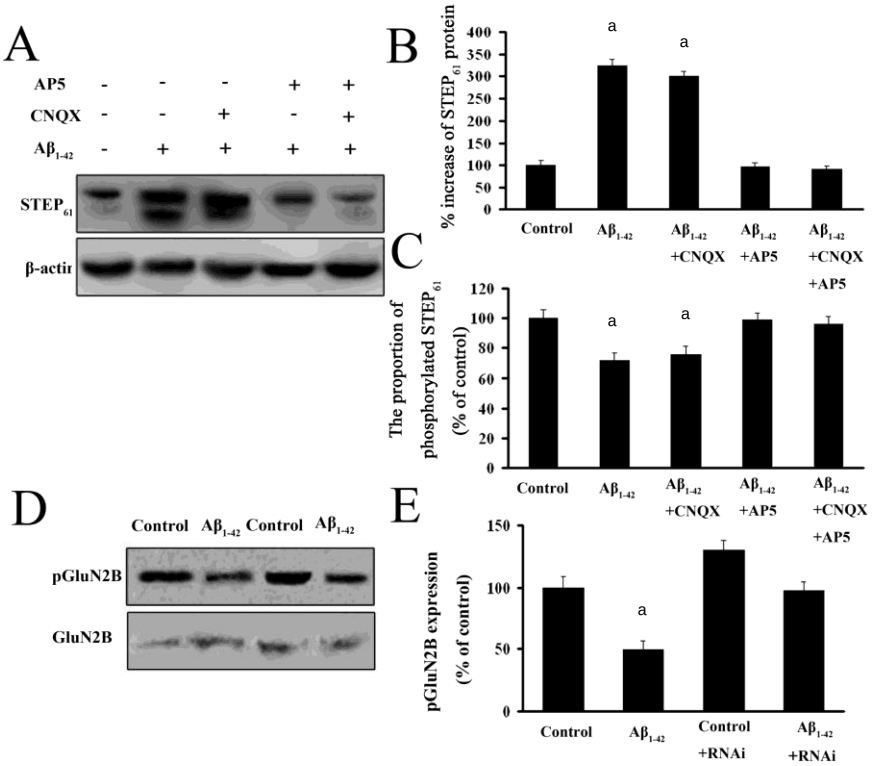

Figure 5 The amyloid-beta ($A\beta_{1–42}$)-induced increase in $STEP_{61}$ levels and the proportion of dephosphorylated $STEP_{61}$ in cortical neurons were mediated by the glutamate/NMDA receptor.

(A) Cortical neurons were pre-incubated with control buffer, NMDA receptor antagonist valeric acid, AP5 (200 μmol/L), non-NMDA receptor antagonist CNQX (20 μmol/L), AP5 + CNQX 10 minutes before 1 μmol/L $A\beta_{1–42}$ treatment for 1 hour and processed to obtain synaptosomes. A western blot was performed for $STEP_{61}$ (61 kDa). The re-probed membrane with β-actin (42 kDa) served as a control for loading.

(B, C) Measurement of STEP61 levels and the proportion of phosphorylated STEP61 after treatment of cultured neurons with control buffer, AP5, CNQX, AP5 + CNQX 10 minutes before $A\beta_{1–42}$ treatment ($^aP < 0.001$, *vs*. control group; mean ± SD of eight mice for each group; one-way analysis of variance and Student-Newman-Keuls *post hoc* tests).

(D) RNAi silencing of $STEP_{61}$ leads to high expression of pGluN2B in cortical neurons cultured in $A\beta_{1-42}$-added medium. The cells were transfected with $STEP_{61}$ siRNA for 48 hours, and western blotting was performed to assess the phosphorylation of GluN2B (pGluN2B; Tyr1472, 190 kDa). Total GluN2B (190 kDa) was not affected. Reprobed membrane with β-actin served as a control for loading.

(E) Quantification of pGluN2B levels from five separate experiments (mean ± SD, $^aP < 0.001$, *vs*. control group; one-way analysis of variance and Student-Newman-Keuls *post hoc* tests of eight mice for each group). All tests were performed at least three times to ensure reproducibility.

$STEP_{61}$: Striatal-enriched phosphatase 61; NMDA: N-methyl-D-aspartate; AP5: valeric acid; CNQX: 6-cyano-T-nitroquinoxaline-2,3-dione.

DISCUSSION

In the present study, we used APP/PS1 mice as an Alzheimer's disease mouse model. The transgenic mice expressed a chimeric mouse/human amyloid precursor protein (Mo/HuAPP695swe) and mutant human presenilin 1 (PS1-dE9). Both mutations are associated with early onset of Alzheimer's disease[17]. The Mo/HuAPP695swe transgene causes mice to secrete a human Aβ peptide. As previously reported, STEP is expressed in both the soma and the processes of all neurons[7]. The present findings revealed elevated $STEP_{61}$ levels in the cortex and hippocampal CA1 region of middle-aged APP/PS1 transgenic mouse brains. We speculated that the increase in $STEP_{61}$ levels is likely caused by increases in Aβ levels or overexpression of the APP or PS1 mutant. In addition, cognitive deficits are normally present in aged APP/PS1 transgenic mice. Therefore, there are possible correlations between $STEP_{61}$ and cognitive deficits in APP/PS1 mice. It has been reported that genetic reduction of STEP in 3xTg-Alzheimer's disease mice results in significant improvements in three cognitive tasks[18]. These findings demonstrate the importance of $STEP_{61}$ in normal cognitive

function, and its possible involvement in cognitive disorders such as Alzheimer's disease.

The behavioral impairments in Alzheimer's disease transgenic mice are consistent with the biochemical data. The pGluN2B level is significantly lowered in the cortex and hippocampus from APP/PS1 transgenic mice. Recent studies have suggested that NMDA receptor mislocalization is a dominant factor contributing to glutamatergic dysfunction and pathogenesis in neurological disorders such as Alzheimer's disease and ischemia. Therapeutic approaches that specifically rectify receptor mislocalization or target downstream apoptotic signaling pathways could be beneficial for preventing disease onset or progression across many disorders that are commonly caused by NMDA receptor dysfunction[19-20]. NMDA receptors are ion channels gated by glutamate; they are widespread in the central nervous system and are involved in numerous physiological and pathological processes including synaptic plasticity, chronic pain and psychosis. Aberrant NMDA receptor activity also plays an important role in the neuronal loss associated with ischemic insults and major degenerative disorders including Parkinson's and Alzheimer's diseases. Agents that target and alter NMDAR function may, thus, have therapeutic benefit[21-23]. Previous studies have shown that $STEP_{61}$ associates with the NMDA receptor complex, reduces NMDA receptor activity, and opposes the induction of long-term potentiation through a process whereby STEP dephosphorylates a regulatory tyrosine site (Tyr1472) on the GluN2B subunit, leading to internalization of GluN1/GluN2B receptor complexes[24-25]. In the present study, the pGluN2B level was significantly decreased in the cortex and hippocampus from APP/PS1 mice, and this decrease was accompanied by an increase in $STEP_{61}$ levels. Decreased pGluN2B levels were also observed in an AD cell model. The changes in $STEP_{61}$ protein level as well as the proportion of dephosphorylated $STEP_{61}$ could possibly be involved in the decreased phosphorylation of GluN2B. Importantly, knockdown of $STEP_{61}$ enhanced the pGluN2B level. It has been reported that phosphorylation of GluN2B at Tyr1472 is correlated positively with NMDA currents[26]. This implies that $STEP_{61}$ is possibly involved in the trafficking of NMDA receptors, and that it is inappropriately activated by Aβ.

Furthermore, we extended these findings by demonstrating a role for NMDA receptors in the pathological pathways affecting $STEP_{61}$ regulation in Alzheimer's disease, which has not previously been reported. Pretreatment with the NMDA receptor antagonist valeric acid (AP5), but not the non-NMDA receptor antagonist CNQX before treatment with $A\beta_{1-42}$ inhibited the increase in STEP levels and activation. Thus, NMDA receptor-mediated Ca^{2+} influx appears to be responsible for the effects of Aβ-induced activation of $STEP_{61}$. Taken together, the results of the present study indicate that $STEP_{61}$ has potential to negatively regulate the activation of GluN2B *via* NMDA receptors that may be associated with the pathology of Alzheimer's disease.

MATERIALS AND METHODS

Design

A randomized, controlled, *in vivo* and *in vitro* study.

Time and setting

The experiments were performed at the Central Laboratory of China Medical University, China from May to November 2011.

Materials

A total of 16 healthy, 12-month-old, male APP/PS1 mice (Shenyang, China; license No. SYXK (Liao) 2008-0005) and age-matched C57BL/6 mice, weighing 30.0 ± 6.5 g, were used. Throughout the experiments, the animals were maintained in stainless-steel cages in a controlled environment (22–25°C, 40–60% relative humidity, 12-hour light-dark cycle), with free access to food and water.

All procedures were performed in accordance with the *Guidance Suggestions for the Care and Use of Laboratory Animals*, formulated by the Ministry of Science and Technology of China[27].

Methods

Morris water maze test for spatial learning and memory deficit in transgenic mice

The apparatus consisted of a circular water tank (120 cm in diameter and 50 cm high). The water was rendered opaque by the addition of nontoxic white paint and the water temperature was maintained at 23 ± 1°C. The mice were required to find the hidden platform using spatial cues available in the testing room. They were given 60 seconds to find the submerged platform. The mice were allowed to stay on the platform for 20 seconds. The time that an individual mouse took to reach the hidden platform was recorded as the escape latency (second). The swimming speed was recorded and analyzed.

The average time that an individual mouse spent in the target quadrant that previously contained the hidden

platform was respectively recorded as a measure of spatial memory. The visible platform tests (four trials per day for 2 days) were performed 24 hours after the probe trial. In this trial, the visible platform was positioned 1 cm above the water surface. The time to reach the visible platform and the percentage of time spent in the correct quadrant were recorded and analyzed.

PCR for detection of APP expression in APP/PS1 transgenic mice

A fragment of the APP gene was amplified by PCR from transgenic mouse tail genomic DNA using Taq DNA polymerase. After initial denaturation at 94°C for 5 minutes, 30 cycles of amplification were performed. DNA was annealed at 55°C for 30 seconds, and the samples were incubated at 72°C for 5 minutes to ensure complete strand extension.

Gene	Sequence (5'–3')	Product size (bp)
APP	Upstream: GAC TGA CCA CTC GAC CAG GTT CTG Downstream: CTT GTA AGT TGG ATT CCT CAT ATC CG	270

Culture of primary cortical neurons from C57BL/6 mice

Primary cortical neuronal cultures were prepared from timed-pregnant E15–16 wild-type (C57BL/6) mice[28]. The brains were removed and the cortices dissected out under a dissecting microscope. Tissue was trypsinized with 0.025% trypsin-ethylenediamine tetraacetic acid (Ybiotech, Shanghai, China) and dissociated in Hanks balanced salt solution (Beyotime, Jiangsu, China) by trituration to isolate cells. Cortical cells were resuspended in neurobasal medium containing B27 supplement and 5% fetal bovine serum (Hyclone, Shanghai, China) and plated in 12-well culture dishes containing poly-D-lysine (Sigma, St. Louis, MO, USA)-coated 18-mm German-glass coverslips. The cells were maintained in neurobasal medium without fetal bovine serum for 14–15 DIV at 37°C in a humidified 5% CO_2 incubator.

Immunohistochemistry for distribution and expression of $STEP_{61}$ in the cortex and hippocampus

Serial coronal sections (5 μmol/L thickness) were cut from various sections of the brain. After the coronal sections were rinsed in PBS three times, citrate buffer was used for endogenous antigen retrieval. Peroxidase activity was blocked by incubation with 3% H_2O_2 for 10 minutes. The sections were incubated with 10% normal goat serum. After the blocking serum was removed, sections were immunostained overnight at 4°C using a rabbit anti-$STEP_{61}$ polyclonal antibody (1:150; Abgent, San Diego, CA, USA), and then with biotinylated secondary antibody goat anti-rabbit IgG at 37°C for 20 minutes (Beijing Zhongshan Biotechnology Co., Ltd.). $STEP_{61}$-positive cells were detected using streptavidin-biotin complex and 3,3'-diaminobenzidine kits (Zhongshan, Beijing, China). Primary antibodies were replaced with PBS buffer as a negative control. Immunohistochemical results were judged by HSCORE (histological score)[29]. The HSCORE was calculated using two indices, proportion (Pí) and intensity (í). The Pí was estimated based on the percentage of positive cells. The í was judged as 0 (no staining), or 1+ (light brown staining), or 2+ (brown staining), or 3+ (heavy brown staining). The $STEP_{61}$ HSCORE was derived by summing the proportion of cells stained at each intensity, multiplied by the intensity of staining.

HSCORE = $\sum$Pí×í, where í = 0, 1, 2 or 3 and Pí varied from 0 to 1.0, $STEP_{61}$ HSCOREs ranged from a minimum of zero in cases with no staining to a maximum of 3.0 in cases in which all the cells stained with maximal intensity. We judged HSCORE > 0 as positive and HSCORE = 0 as negative. HSCORE ≥ 2.0 was judged as highly positive. In each $STEP_{61}$ section, the stained cells were counted in three visual fields (n = 5) from each of the cortex and hippocampal CA1 regions.

Preparation of synaptosomes from cortex and hippocampus

Homogenates were prepared from brain tissue using glass homogenizers in homogenization buffer: 0.35 mol/L sucrose, 10 mmol/L Tris, 0.5 mmol/L EGTA solution brought to pH 7.4 with KOH. The homogenates were centrifuged at 2 000 × g for 1 minute on a Beckman model J-21B centrifuge using a JA-20 fixed angle rotor to remove the nuclear pellet (Pl). Pl was washed once by resuspension in the homogenizing buffer and repelleted. The supernatant was combined with the supernatant from the first centrifugation, and the pellet was discarded. The pooled supernatant (Sl) was centrifuged at 23 000 × g for 4 minutes to yield a crude mitochondrial pellet (P2), which was washed once by resuspension in homogenizing buffer and repelleted. The pellet was then brought up to 6 mL total volume with the same buffer. This suspension was layered onto a discontinuous gradient of 5% and 13% Ficoll in 0.35 mol/L sucrose (1 mL suspension/2 mL each of 5 and 13% Ficoll) that had been allowed to equilibrate at 4°C for 1 hour prior to loading the sample. The gradient was centrifuged at 45 000 × g 45 minutes on a Beckman L5-75 ultracentrifuge (Oregon, USA) using an SW 50.1 swinging bucket rotor. A synaptosomal fraction was collected from the 5–13% interface and

washed by diluting in 0.35 mol/L sucrose/10 mmol/L Tris and centrifuging at 23 000 × *g* for 20 minutes. The synaptosomal pellet was resuspended in incubation buffer[30].

Assessment of cell viability by MTT assay

Cell viability was measured in 96-well plates by quantitative colorimetric assay with MTT (KeyGEN Biotech, Nanjing, China), which is an indicator of the mitochondrial activity of living cells. Cell viability was expressed as the ratio of the signal obtained from treated cultures and control cultures.

Quantitative real-time reverse transcription-PCR

1 μg of total RNA was reverse transcribed to cDNA in a total volume of 20 μL using an RT (reverse transcriptase) reaction kit (TaKaRa, Tokyo, Japan). Real-time PCR was performed using a Thermal Cycler Dice® real-time system (TaKaRa Code: TP800) according to the manufacturer's instruction and SYBR® Premix Ex Taq (TaKaRa) as a DNA-specific fluorescent dye. PCR was carried out for 45 cycles of 95°C for 5 seconds and 60°C for 30 seconds. All reactions were repeated at least three times. The primers used for analysis of β-actin mRNA are as follows:

Gene	Gene sequence (5'–3')	T_m (°C)	Product size (bp)
$STEP_{61}$	Upstream: TTC CTA CAT CAA TGC CAA CTA C Downstream: GCT CCT CCG GCC AAT AC	55.0	194
β-actin	Upstream: TCG TGC GTG ACA TTA AGG AG Downstream: ATG CCA GGG TAC ATG GTG GT	55.0	304

T_m: Temperature.

Western blot analysis for $STEP_{61}$, pGluN2B and GluN2B protein expression in the cortex and hippocampus

Protein concentrations were determined by bicinchoninic acid assay. Membrane proteins (100 μg for each sample) were subjected to sodium dodecyl sulfate polyacrylamide gel electrophoresis using 10% gradient Tris/glycine gels. Then, proteins were transferred to polyvinylidene difluoride membrane (Millipore, Temecula, CA, USA). Blots were incubated with the following primary antibodies: rabbit polyclonal anti-$STEP_{61}$ (1:300; Abgent, San Diego, CA, USA), rabbit anti-pGluN2B, -GluN2B polyclonal antibody (1:500; Cell Signaling Technology, Beverly, MA, USA), and rabbit anti-β-actin monoclonal antibody (1:500; Biosynthesis Biotechnology Co., Beijing, China). The samples were detected using a chemiluminescent detection system (Pierce Technology, Rockford, IL, USA), and the absorbance of each band was measured using Image J software (Chicago, IL, USA). Western blot was performed at least three times to ensure reproducibility.

Statistics analysis

Data were expressed as mean ± SD and were analyzed by one-way analysis of variance and Student-Newman-Keuls *post hoc* test using SPSS 18.0 software (SPSS, Chicago, IL, USA). Differences were considered statistically significant if the *P* value was less than 0.05.

REFERENCES

[1] Donmez G. The effects of SIRT1 on Alzheimer's disease models. Int J Alzheimers Dis. 2012;2012(3):509-529.

[2] Hardy J, Selkoe DJ. The amyloid hypothesis of Alzheimer's disease: progress and problems on the road to therapeutics. Science. 2002;297(5580):353-356.

[3] Venkitaramani DV, Paul S, Zhang Y, et al. Knockout of striatal enriched protein tyrosine phosphatase in mice results in increased ERK1/2 phosphorylation. Synapse. 2009;63(1):69-81.

[4] Terry RD, Masliah E, Salmon DP, et al. Physical basis of cognitive alterations in Alzheimer's disease: synapse loss is the major correlate of cognitive impairment. Ann Neurol. 1991;30(4):572-580.

[5] Lombroso PJ, Murdoch G, Lerner M. Molecular characterization of a protein-tyrosine-phosphatase enriched in striatum. Proc Natl Acad Sci U S A. 1991;88(16):7242-7246.

[6] Paul S, Snyder GL, Yokakura H, et al. The Dopamine/D1 receptor mediates the phosphorylation and inactivation of the protein tyrosine phosphatase STEP via a PKA- dependent pathway. J Neurosci. 2000;20(15): 5630-5638.

[7] Paul S, Nairn AC, Wang P, et al. NMDA-mediated activation of the tyrosine phosphatase STEP regulates the duration of ERK signaling. Nat Neurosci. 2003;6(1):34-42.

[8] Adams JP, Sweatt JD. Molecular psychology: roles for the ERK MAP kinase cascade in memory. Annu. Rev Pharmacol Toxicol. 2002;42:135-163.

[9] Baum ML, Kurup P, Xu J, et al. A STEP forward in neural function and degeneration. Commun Integr Biol. 2010;3(5):419-422.

[10] Pelkey K, Askalan R, Paul S, et al. Tyrosine phosphatase STEP is a tonic brake on induction of long-term potentiation. Neuron. 2002;34(1):127-138.

[11] Carty NC, Xu J, Kurup P, et al. The tyrosine phosphatase STEP: implications in schizophrenia and the molecular mechanism underlying antipsychotic medications. Transl Psychiatry. 2012;10(2):e137.

[12] Ferreira IL, Bajouco LM, Mota SI, et al. Amyloid beta peptide 1-42 disturbs intracellular calcium homeostasis through activation of GluN2B-containing N-methyl-d-aspartate receptors in cortical cultures. Cell Calcium. 2012;51(2):95-106.

[13] Mori H, Mishina M. Structure and function of the NMDA receptor channel. Neuropharmacology. 1995;34(10): 1219-1237.
[14] Moon IS, Apperson ML, Kennedy MB. The major tyrosinephosphorylated protein in the postsynaptic density fraction is N-methyl-D-aspartate receptor subunit 2B. Proc Natl Acad Sci U S A. 1994;91(9):3954-3958.
[15] Nakajima A, Kinugasa Y, Torii J, et al. Repeated treatment with nicotine induces phosphorylation of NMDA receptor NR2B subunit in the brain regions involved in behavioral sensitization. Neurosci Lett. 2012;524(2):133-138.
[16] Sonkusare SK, Kaul CL, Ramarao P. Dementia of Alzheimer's disease and other neurodegenerative disorders--memantine, a new hope. Pharmacol Res. 2005; 51(1):1-17.
[17] Ruan L, Kang Z, Pei G, et al. Amyloid deposition and inflammation in APPswe/PS1dE9 mouse model of Alzheimer's disease. Curr Alzheimer Res. 2009; 6(6): 531-540.
[18] Zhang Y, Kurup P, Xu J, et al. Genetic reduction of striatal-enriched tyrosine phosphatase (STEP) reverses cognitive and cellular deficits in an Alzheimer's disease mouse model. Proc Natl Acad Sci U S A. 2010;107(44): 19014-19019.
[19] Gladding CM, Raymond LA. Mechanisms underlying NMDA receptor synaptic/extrasynaptic distribution and function. Mol Cell Neurosci. 2011;48(4):308-320.
[20] Groc L, Bard L, Choquet D. Surface trafficking of N-methyl-D-aspartate receptors: physiological and pathological perspectives. Neuroscience. 2009;158(1): 4-18.
[21] Mony L, Kew JN, Gunthorpe MJ, et al. Allosteric modulators of NR2B-containing NMDA receptors: molecular mechanisms and therapeutic potential. Br J Pharmacol. 2009;157(8):1301-1317.
[22] Lopez de Armentia M, Sah P. Development and subunit composition of synaptic NMDA receptors in the amygdala: NR2B synapses in the adult central amygdala. J Neurosci. 2003;23(17):6876-6883.
[23] Ye GL, Yi S, Gamkrelidze G, et al. AMPA and NMDA receptor-mediated currents in developing dentate gyrus granule cells. Brain Res Dev Brain Res. 2005;155(1): 26-32.
[24] Kurup P, Zhang YF, Xu J, et al. Aβ-mediated NMDA receptor endocytosis in Alzheimer's disease involves ubiquitination of the tyrosine phosphatase STEP61. J Neurosci. 2010;30(17):5948-5957.
[25] Chin J, Palop JJ, Puolivali J, et al. Fyn kinase induces synaptic and cognitive impairments in a transgenic mouse model of Alzheimer's disease. J Neurosci. 2005;25(42): 9694-9703.
[26] Alvestad RM, Grosshans DR, Coultrap SJ, et al. Tyrosine dephosphorylation and ethanol inhibition of N-methyl-Daspartate receptor function. J Biol Chem. 2003; 278(13): 11020-11025.
[27] The Ministry of Science and Technology of the People's Republic of China. Guidance Suggestions for the Care and Use of Laboratory Animals. 2006-09-30.
[28] Venkitaramani DV, Paul S, Zhang Y, et al. Knockout of striatal enriched protein tyrosine phosphatase in mice results in increased ERK1/2 phosphorylation. Synapse. 2009;63(1):69-81.
[29] Plante BJ, Kannan A, Bagchi MK, et al. Cyclic regulation of transcription factor C/EBP beta in human endometrium. Reprod Biol Endocrinol. 2009;17(7):15.
[30] Frank AW, Randy JA, Fengju BA. Proteomic survey of rat cerebral cortical synaptosomes. Proteomics. 2005;5(8): 2177-2201.

(Reviewed by McGowan D, Frenchman B, Xie JW, Xu J)
(Edited by Wang J, Su LL, Li CH, Song LP, Liu WJ, Zhao M)